Journal of
Experimental
Botany

www.jxb.oxfordjournals.org

RESEARCH PAPER

A somaclonal line *SE7* of finger millet (*Eleusine coracana*) exhibits modified cytokinin homeostasis and increased grain yield

Volodymyr Radchuk[1,*], Ruslana Radchuk[1], Yaroslav Pirko[1,2], Radomira Vankova[3], Alena Gaudinova[3], Vitaly Korkhovoy[1,2], Alla Yemets[2], Hans Weber[1], Winfriede Weschke[1] and Yaroslav B. Blume[2]

[1] Leibniz Institute of Plant Genetics and Crop Plant Research (IPK), Corrensstrasse 3, D-06466 Gatersleben, Germany

[2] Institute of Food Biotechnology and Genomics, National Academy of Science of Ukraine, Osipovskogo Str. 2a, 04123 Kiev, Ukraine

[3] Laboratory of Hormonal Regulations in Plants, Institute of Experimental Botany, Academy of Sciences of the Czech Republic, Rozvojová 263, 16502 Prague 6, Czech Republic

* To whom correspondence should be addressed. E-mail: radchukv@ipk-gatersleben.de

Abstract

The *SE7* somaclonal line of finger millet (*Eleusine coracana*) achieved increased grain yield in field trials that apparently resulted from a higher number of inflorescences and seeds per plant, compared with the wild type. Levels of endogenous cytokinins, especially those of highly physiologically active *iso*-pentenyl adenine, were increased during early inflorescence development in *SE7* plants. Transcript levels of cytokinin-degrading enzymes but not of a cytokinin-synthesizing enzyme were also decreased in young leaves, seedlings, and initiating inflorescences of *SE7*. These data suggest that attenuated degradation of cytokinins in *SE7* inflorescences leads to higher cytokinin levels that stimulate meristem activity and result in production of more inflorescences. Gene expression was compared between *SE7* and wild-type young inflorescences using the barley 12K cDNA array. The largest fraction of up-regulated genes in *SE7* was related to transcription, translation, and cell proliferation, cell wall assembly/biosynthesis, and to growth regulation of young and meristematic tissues including floral formation. Other up-regulated genes were associated with protein and lipid degradation and mitochondrial energy production. Down-regulated genes were related to pathogen defence and stress response, primary metabolism, glycolysis, and the C:N balance. The results indicate a prolonged proliferation phase in *SE7* young inflorescences characterized by up-regulated protein synthesis, cytokinesis, floral formation, and energy production. In contrast, wild-type inflorescences are similar to a more differentiated status characterized by regulated protein degradation, cell elongation, and defence/stress responses. It is concluded that attenuated degradation of cytokinins in *SE7* inflorescences leads to higher cytokinin levels, which stimulate meristem activity, inflorescence formation, and seed set.

Key words: Cytokinin, cytokinin metabolism, finger millet, gene expression, inflorescence development, somaclonal variation.

Introduction

Grain yield of crop plants largely depends on grain number per plant, which is correlated with the number of inflorescences formed in the meristems. To understand the mechanisms, which determine and control meristem differentiation is economically relevant, and enhanced inflorescence formation is important to maximize yield potential.

The balance between meristem maintenance and differentiation is mediated by auxin to cytokinin (CK) ratios (Barazesh

and McSteen, 2008). CK deficiency diminishes the activity of vegetative and floral shoot apical meristems, indicating an absolute CK requirement for stimulation of cell division (Werner *et al.*, 2003). CK levels depend on *de novo* synthesis, conjugation, and degradation, as well as on local and long-distance transport. Thereby, a precise CK homeostasis is maintained within a certain organ (Kudo *et al.*, 2010). The CK biosynthesis pathway and the participating key genes have been identified (Kamada-Nobusada and Sakakibara, 2009; Frebort *et al.*, 2011). Adenosine phosphate-*iso*-pentenyltransferase (IPT) catalyses the initial step of N^6-(Δ^2-isopentenyl) adenine (iP) and *trans*-zeatin (tZ) biosynthesis utilizing dimethylallyl diphosphate (DMAPP) and ATP/ADP to generate iP-ribotides (Sakamoto *et al.*, 2006). iP-ribotides are hydroxylated to tZ-ribotides by cytokinin *trans*-hydroxylase (CYP735A; Takei *et al.*, 2004). tRNA iso-pentenyltransferase (tRNA-IPT) synthesizes *cis*-zeatin (cZ; Miyawaki *et al.*, 2006). Conversion of iP-, tZ-, and cZ-ribotide 5′-monophosphate to active forms may occur by two-step activation. In this pathway, ribotides are dephosphorylated to ribosides and converted to free-base CKs (Kudo *et al.*, 2010). The genes involved, however, have not been identified. In the direct activation pathway (Kuroha *et al.*, 2009; Tokunaga *et al.*, 2012), CK ribotide 5′-monophosphates are converted to free-base CKs by cytokinin nucleoside 5′-monophosphate phosphoribohydrolase, also called LONELY GUY (LOG; Kurakawa *et al.*, 2007). CK is degraded by cytokinin oxidase/dehydrogenase (CKX; Galuszka *et al.*, 2001; Schmülling *et al.*, 2003), which is important for regulation of CK activity. Plants perceive and respond to CKs through two-component systems (Werner and Schmülling, 2009; Perilli *et al.*, 2010; Müller, 2011) consisting of CK receptors and response regulators. Enzymes involved in CK biosynthesis, perception, and degradation are generally encoded by gene families (Müller, 2011).

Local CK biosynthesis within the meristem in rice is essential, as shown for *log* mutants encoding a CK biosynthesis gene. *LOG* loss-of-function mutants exhibit reduced CK levels and panicle size, branching, and numbers of flowers and stamens (Kurakawa *et al.*, 2007). On the other hand, *CKX* loss of function results in increased CK levels and seed set in cereals (Ashikari *et al.*, 2005; Zalewski *et al.*, 2010) and *Arabidopsis* (Bartrina *et al.*, 2011). CKs can affect different metabolic pathways stimulating assimilate transporters for nitrate, ammonium, sulphate, phosphate, and iron (Sakakibara, 2006; Séguéla *et al.*, 2008; Werner *et al.*, 2010). In barley, CKs participate in regulation of grain size, possibly by influencing both the accumulation and the duration of the filling period (Mechael and Seiler-Kelbitsch, 1972).

Finger millet [*Eleusine coracana* (L.) Gaerth.] is an ancient crop plant cultivated mainly as a cereal in the arid areas of Africa and Asia. *Eleusine coracana* is originally native to the Ethiopian Highlands and was introduced into India ~4000 years ago. It is very adaptable to higher elevations and is grown in the Himalaya up to 2300 m in elevation. It is estimated that finger millet is grown on ~38000 km^2 of land (http://en.wikipedia.org/wiki/Eleusine_coracana). Due its ability to grow in semi-arid regions, tolerance to severe diseases, its nutritional values (especially a high methionine content), and good storage properties of grains, *E. coracana* can become an attractive crop in sustainable agriculture of developing countries contributing to a secure food resource. However, genetic characterization of finger millet is just beginning. Construction of genetic maps has been initiated (Dida *et al.*, 2007) and comparative analysis revealed high levels of co-linearity between finger millet and rice genomes (Srinivasachary *et al.*, 2007). Recently, a transformation protocol has been published for finger millet (Ceasar and Ignacimuthu, 2011).

In this work, the somaclonal line *SE7* of finger millet, which exhibits decreased plant height and considerably increased grain yield compared with the wild type, is reported. Increased CK levels were found during early flower development together with decreased amounts of *CKX* transcripts. This suggests attenuated degradation of CKs in *SE7* inflorescences resulting in higher levels of CKs, which stimulate meristem activity, inflorescence formation, and seed set.

Materials and methods

Plant materials

Field evaluation of the phenotype was done using ~100 wild-type (variety Tropikanka) and *SE7* finger millet plants, grown for 2 weeks in a greenhouse and then transplanted into the field in Gatersleben, Germany in May 2011 with 20 cm × 20 cm distances between single plants. Plant height and yield from 25 plants were measured in late September 2011. For metabolite and array analyses, whole developing inflorescences were collected (Fig. 3A). For quantitative reverse transcription-PCR (qRT-PCR) analyses of different tissues, total RNA was isolated form seedlings at 5 d after imbibition, young leaves at the tillering stage, and old leaves from maturating plants. All samples were collected at least in triplicate from biologically independent plant material.

Cloning of the cDNA for genes involved in cytokinin metabolism

Total RNA was extracted from different tissues of the wild type and the *SE7* mutant of finger millet using Trizol reagent (Invitrogen). For this, 100 mg of tissue was ground in liquid nitrogen, mixed with 1 ml of pre-heated Trizol (60 °C) for 5 min, and centrifuged at 13000 rpm for 10 min at 4 °C. The supernatant was transferred into a new tube, mixed with 0.2 ml of chloroform for 2 min, and centrifuged at 13000 rpm for 10 min at 4 °C. The aqueous phase was transferred into a new tube and mixed with 0.6 vol. of *iso*-propanol, left at room temperature for 10 min, and then centrifuged at 13 000 rpm for 10 min at 4 °C. The pellet was rinsed once with 70% cold ethanol and dissolved in 100 μl of distilled water. The isolated RNA was treated with RNase-free DNase (Qiagen), purified using an RNeasy plant mini kit (Qiagen), and used for the synthesis of cDNA, quantitative RT-PCRs, and cDNA array.

cDNA fragments of the *CKX*, *LOG*, and *CYTOKININ RESPONSE 1* (*CRE1*) genes were amplified from wild-type inflorescences of finger millet by RT-PCRs using gene-specific primers selected from conserved regions of the corresponding rice genes. Primers used for RT-PCRs are listed in Supplementary Table S1 available at *JXB* online. All synthesized cDNAs were cloned into the pGEM-T easy vector (Promega) and sequenced. Sequence analysis and alignment were performed using DNAstar. The phylogenetic tree construction was drawn with the ClustalW tool.

Cytokinin extraction and purification

CKs were extracted from 500 μg of corresponding tissue (fresh weight) and purified according to Dobrev and Kaminek (2002). For analyses, 50 pmol of each of the following 17 deuterium-labelled standards were added: [^{2}H$_5$]Z, [^{2}H$_5$]Z9R, [^{2}H$_5$]Z7G, [^{2}H$_5$]Z9G, [^{2}H$_5$]ZOG, [^{2}H$_5$]Z9ROG, [^{2}H$_6$]iP, [^{2}H$_6$]iP9R, [^{2}H$_6$]iP7G, [^{2}H$_6$]iP9G, [^{2}H$_3$]DHZ, [^{2}H$_3$]DHZ9R, [^{2}H$_3$]DHZ9G, [^{2}H$_7$]DHZOG, [^{2}H$_5$]Z9RP, [^{2}H$_6$]iP9RP, and [^{2}H$_3$]DHZ9R (Apex Organics, Honiton, UK). Derivatives of cZ were determined from the retention time and the mass spectra of unlabelled

standards and the response ratio of their tZ counterparts. Briefly, after homogenization in liquid nitrogen, samples were mixed with modified Bieleski solution [MeOH:water:COOH pH 2.5 (15:4:1, v/v/v), –20 °C]. The internal standards were added immediately. After overnight extraction at –20 °C, samples were purified using reverse phase chromatography. The nucleotide fraction was separated from the second fraction containing CK bases, ribosides, and glucosides by ion exchange chromatography (Oasis MCX extraction columns, 6 cc/150 mg, Waters). The nucleotide fraction was treated with alkaline phosphatase and then analysed in the same way as above.

High-performance liquid chromatography/mass spectrometry

High-performance liquid chromatography/mass spectrometry (HPLC/MS) analysis was performed as described by Dobrev *et al*. (2002) using an HPLC/MS system consisting of an HTS-Pal auto-sampler with a cooled sample stack (CTC Analytics, Zwingen, Switzerland), a quaternary HPLC pump Rheos 2200 (Flux Instruments, Basel, Switzerland), a Delta Chrom CTC 100 Column oven (Watrex, Praha, Czech Republic), and a TSQ Quantum Ultra AM triple-quad high resolution mass spectrometer (Thermo Electron, San Jose, CA, USA). Ternary gradient elution (water/acetonitrile/acetic acid) was used. The mass spectrometer was operated in the positive MS/MS mode (SRM; single reaction monitoring) with monitoring of 2–4 transitions for each compound. The most intensive ion was used for quantification and the remainder for identity confirmation. Multilevel calibration graphs with ^{2}H-labelled CK internal standards were used for quantification. Detection limits of different CKs varied from 0.05 pmol to 0.1 pmol per sample. Each sample was injected at least twice.

Quantitative RT-PCR analyses

For qRT-PCR, 5 µg of the total RNA isolated as described above were used for reverse transcription by SuperScript III reverse transcriptase (Invitrogen) with an oligo(dT) primer. The resulting cDNAs were used as template for qRT-PCR analyses which were performed as described earlier (Radchuk *et al*., 2011). The efficiencies of PCRs were estimated using the LinRegPCR software (Ramakers *et al*., 2003). Primer sets for each gene have been selected based on the recommendations by Udvardi *et al*. (2008) and are listed in Supplementary Table S1 at *JXB* online. All samples were run in biological triplicates for each experiment. Dissociation curves confirmed the presence of a single amplicon in each PCR. The Ct of each gene of interest (GOI) from each sample was normalized against the endogenous reference gene actin from finger millet by using the formula $\Delta Ct = Ct_{GOI} - Ct_{actin}$ and calculated as an arithmetic mean of the replicates. In order to highlight the relative gene expression levels in *SE7* versus the wild type, the fold changes of gene expression values were presented as $2^{-\Delta\Delta Ct}$ according to Livak and Schmittgen (2001), where $\Delta\Delta Ct$ is the difference between ΔCt_{WT} and ΔCt_{SE7}.

cDNA array and data analysis

For cDNA array analysis, total RNA was extracted as described above from very early developing inflorescences (stage A, see Fig. 3A) of wild-type and *SE7* finger millet and used for the synthesis of [^{33}P]dCTP-labelled probes. Probe preparation, hybridization, and processing of the 12K barley seed cDNA array was done essentially as described (Sreenivasulu *et al*., 2006) except for the hybridization temperature. In order to increase cross-hybridization between finger millet probes and the barley array, the hybridization temperature was set to 60 °C. Images of hybridized nylon membranes were subjected to automatic spot detection using the MATLAB program. Signal intensities of 11 787 genes were scored from the double spots, enabling the assessment of two replications. Additionally, two biological repetitions were performed using RNA from independently grown plants. Quantile normalization (Bolstad *et al*., 2003) was carried out on the complete data set. Fold changes between wild-type and mutant probes were calculated from the replicates. *P*-values were calculated based on the moderated *t*-test to detect false positives. Genes that showed statistically significant differences in expression in *SE7* in comparison with wild-type inflorescences at the level of ≥1.5-fold

were selected for further analyses. The detailed set of the normalized values, fold difference, and *P*-values of differentially expressed genes are provided in Supplementary Table S2 at *JXB* online.

Accession numbers

Sequence data from this article can be found in the GenBank/EMBL databases under the following accession numbers: HE800184 (*EcCKX1*), HE800185 (*EcCKX2*), HE800186 (*EcLOG1*), HE800187 (*EcCRE1*), and HE800188 (*Ec actin*).

Results

Phenotypic analysis of somaclonal variant SE7 of finger millet

The somaclonal line *SE7* of finger millet [*E. coracana* (L.) Gaertn.] was selected after *in vitro* regeneration of var. Tropikanka (Yemets *et al*., 2003) due to its higher seed yield and more rapid germination at low temperature compared with the initial variety (Baer *et al*., 2007). These agricultural traits were stably inherited over >5 generations.

Phenotypic analyses of the somaclonal line *SE7* under field conditions revealed lower plant height and increased number of tillers per plant compared with the wild type (Fig. 1). To analyse yield-related parameters, field trials were performed in plots of 100 plants planted 20 cm apart. In the plots, the plant height of *SE7* was 10% lower compared with the wild type. Grain yield per plant was increased by 40% and total tiller number was 17% higher. The number of grains per plant was also increased by 40%, while the 100 grain weight was unchanged (Fig. 2). The results show that the *SE7* line under field conditions has achieved considerably higher grain yield, which was probably caused by a higher seed number due to an increased number of tillers per plant.
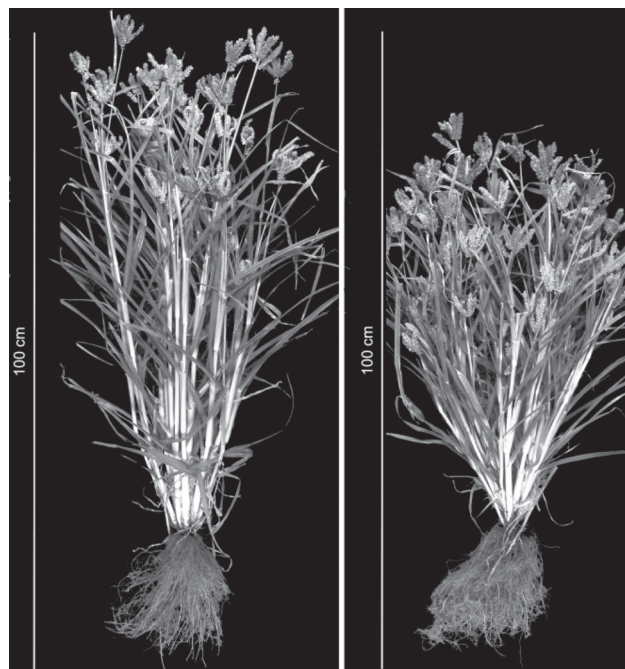

Fig. 1. Lower plant height and increased number of inflorescences in the somaclonal line *SE7* (right) compared with the wild-type finger millet (left).
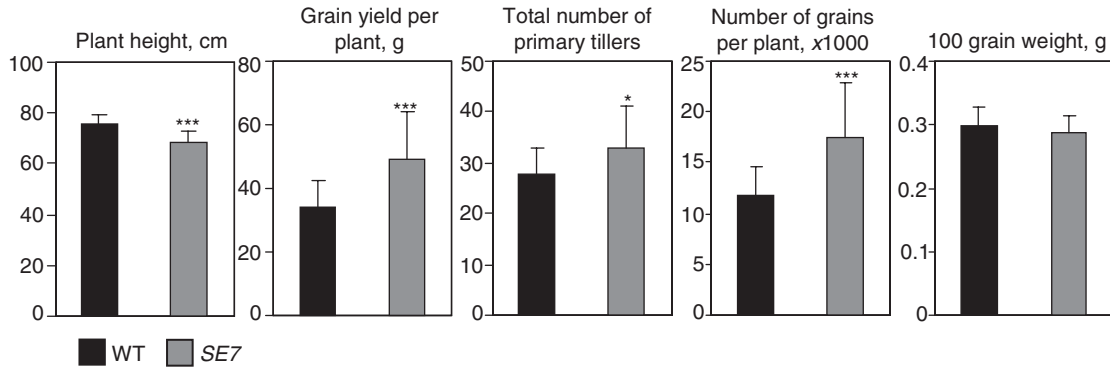
Fig. 2. Phenotypic analysis of field-grown *SE7* plants compared with wild-type finger millet. Each bar represents the mean values ±SD of a trait. Significant differences between the mutant and wild type, calculated by Student's *t*-test are: *$P < 0.05$; and ***$P < 0.001$.

Cytokinin contents in developing inflorescences of SE7 *and wild-type finger millet*

The higher number of inflorescences formed in the *SE7* line indicates that more generative/floral spikes were produced in the meristems. Such an increased meristematic activity is often caused by modified levels of phytohormones, especially of CKs (Ashikari *et al.*, 2005; Bartrina *et al.*, 2011). Therefore, endogenous levels of 16 CK derivatives were measured in the inflorescences of *SE7* and the wild type at two developmental stages: flower initiation with total inflorescence lengths <1 cm and flower development with inflorescence length between 1 cm and 3 cm (Fig. 3A). Significantly different levels were measured only at the stage of flower initiation (Fig. 3B) but not during flower development (Supplementary Fig. S1 at *JXB* online).

The active CK pool included predominantly iP (Fig. 3B). In *SE7* inflorescences, iP levels were as much as 14-fold higher compared with the wild type. The amounts of tZ and dihydrozeatin (DZ) were almost not detectable. Levels of iP riboside-phosphate (iPRP) were 30% higher in *SE7*, whereas that of the nucleoside form, iP riboside (iPR), was 60% lower. Levels of the iP deactivation product, iP 9-glucoside (iPN9G), were also decreased in the *SE7* line, although not significantly. Amounts of tZ were barely detectable in early inflorescences, whereas levels of tZ precursors and the riboside forms, tZRP and tZR, did not differ between *SE7* and the wild type. Levels of cZ were barely detectable, whereas those of cZRP and cZR were increased by 2- and 3-fold (Fig. 3B).

The CK measurement revealed increased levels of several derivatives, especially of the highly physiologically active iP in initiating inflorescences of the *SE7* mutant finger millet. Such changes could be affected by altered expression of genes related to CK metabolism.

Cloning of genes involved in cytokinin metabolism and perception

To elucidate whether altered endogenous CK levels in the *SE7* mutant were caused by differential expression of genes involved in CK metabolism and/or perception, the corresponding cDNAs were cloned from finger millet. As little sequence information is available for finger millet, cDNA fragments were PCR amplified from early developing inflorescences using primers from conserved regions of known rice and barley homologues. For CKX, 10 barley genomic and corresponding cDNA sequences (Matsumoto *et al.*, 2011; Mameaux *et al.*, 2012) and 11 rice (Ashikara *et al.*, 2005) cDNAs were examined. Sequences for barley and rice LOG have not been described and were therefore selected from available full-length cDNA and expressed sequence tag (EST) collections according to homology (Zhang *et al.*, 2004; Kuroha *et al.*, 2009; Matsumoto *et al.*, 2011). Five full-length barley *LOG* cDNAs were identified. The rice genome contains all four counterparts of *Arabidopsis* hybrid kinases (HKs) (Supplementary Fig. S2 at *JXB* online). In addition, one full-length *HvHK3* and one partial *HvCRE1* cDNA of barley were identified.

Differences in CK levels between the wild type and *SE7* were measured at initiation (stage A) of inflorescence development (Fig. 3A). Therefore, total RNA from this stage was used to amplify cDNA fragments by RT-PCR. The 1411 bp *EcCKX1* fragment is 61.8% identical to *Arabidopsis AtCKX6*, 86.6% identical to barley *HvCKX4*, and 84.6% identical to rice *OsCKX4* at the amino acid level. The 1758 bp *EcCKX2* fragment is 83.8% identical to *OsCKX3*, 77.7% identical to *HvCKX3*, and 44.6% identical to *AtCKX1* (Supplementary Fig. 2A at *JXB* online). The 957 bp *EcLOG1* fragment is 78.7% identical to *HvLOG4* and 78.4% identical to *OsLOG4* (Supplementary Fig. 2B). The *EcCRE1* fragment of 706 bp contains conserved receptor-like (RLD) and receiver domains with highly conserved aspartate residues and is 68.8% identical to *OsCRE1*, 61.1% identical to *HvCRE1*, and 42.7% identical to *CRE1/WOL1/AHK4* of *Arabidopsis* (Supplementary Fig. 2C). Further members of *CKX*, *LOG*, or *HK* gene families could not been cloned, possibly due to absent transcripts in early inflorescences or to unsuitable primers selected for amplification. Differential temporal and spatial expression patterns for the particular members of these gene families have been described previously (Werner *et al.*, 2003; Zalewski *et al.*, 2010; Tokunaga *et al.*, 2012).

Corresponding fragments of *EcCKX1*, *EcCKX2*, *EcLOG1*, and *EcCRE1* cDNAs were also amplified from inflorescences of the line *SE7*. The sequences in the wild type and *SE7* were not different. This indicates that changed expression rather than the sequence structure of CK-related genes may alter CK levels in the *SE7* line.
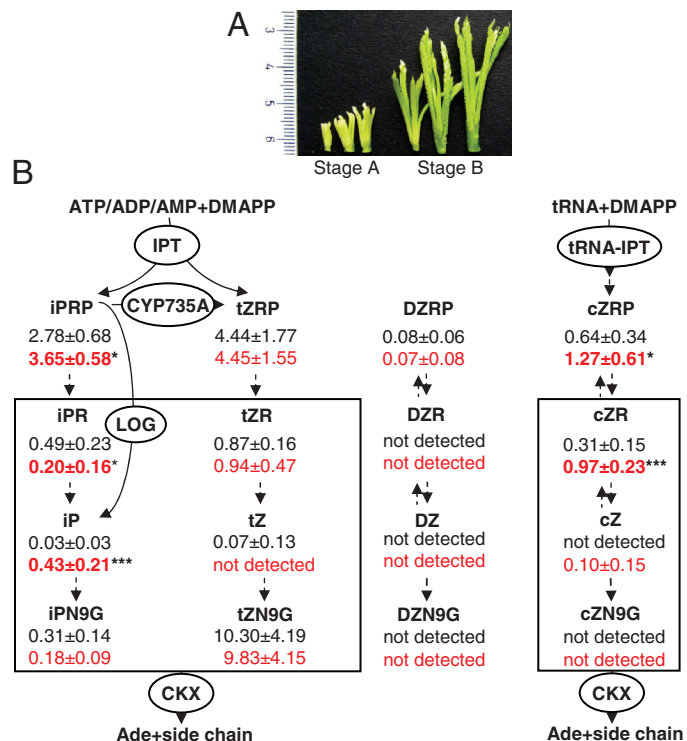
Fig. 3. (A) General view of developing finger millet inflorescences used for cytokinin measurements as well as for molecular biological analyses. (B) Levels of cytokinins measured in young inflorescences (stage A) of *SE7* and wild-type finger millet. Wild-type cytokinin contents are depicted in black; and those of the *SE7* mutant in red. Data represent mean values (in pmol g^{-1} fresh weight) ±SD. Values representing significant differences between *SE7* and the wild type are shown in bold (*$P < 0.05$; ***$P < 0.001$, calculated by Student's *t*-test). Key enzymes involved in cytokinin biosynthesis and degradation are shown in circles. Cytokinin derivatives shown in a box are potential targets for the CKX enzyme (Frébort *et al.*, 2011). CKX, cytokinin oxidase/dehydrogenase; cZ, *cis*-zeatin; cZNG, *cis*-zeatin 9-glucoside; cZR, *cis*-zeatin riboside; cZRP, *cis*-zeatin ribotide-phosphate; DZ, dihydro-zeatin; DZNG, dihydro-zeatin 9-glucoside; DZR, dihydro-zeatin riboside; DZRP, dihydro-zeatin ribotide-phosphate; iP, N^6-(Δ^2-isopentenyl) adenine; iPR, iP riboside; iPNG, iP 9-glucoside; iPRP, iP ribotide-phosphate; IPT, adenosine phosphate-isopentenyltransferase; LOG, LONELY GUY; tRNA-IPT, tRNA isopentenyltransferase; tZ, *trans*-zeatin; tZNG, *trans*-zeatin 9-glucoside; tZR; *trans*-zeatin riboside; tZRP, *trans*-zeatin ribotide-phosphate.

Genes involved in cytokinin degradation are down-regulated in SE7 *finger millet*

Expression of *EcCKX1*, *EcCKX2*, *EcLOG1*, and *EcCRE1* genes was analysed in different tissues of *SE7* and the wild type by qRT-PCR. Remarkably, gene expression of *EcCKX2* was 8.2-fold lower in young leaves of *SE7* compared with the wild type. The mRNA levels of *EcCKX1* were 3.9-fold lower in inflorescences of *SE*7 at stage A but unchanged at later stages. Transcript levels of *EcCKX1* and *EcCKX2* genes were lower by 3.2- and 3.1-fold in seedlings but unchanged in mature leaves. The mRNA levels

of *EcLOG1*, encoding a CK-synthesizing enzyme, were undetectable in leaves and unchanged in seedlings. *EcCRE1* transcript levels were 3.9-fold lower in young leaves but unchanged in older leaves and inflorescences (Fig. 4).

In summary, transcript levels of CK-degrading enzymes but not of the CK-synthesizing enzyme were decreased in young and actively growing tissues such as young leaves, seedlings, and initiating inflorescences of *SE7* compared with the wild type. This suggests attenuated degradation of CKs in *SE7* inflorescences relative to the wild type, which is correlated with higher CK levels.

Transcript profiling of early inflorescences of the SE7 *mutant finger millet*

Comparison of gene expression patterns between developing inflorescences of *SE7* and the wild type (Supplementary Table S2 at *JXB* online) was performed using the barley seed-specific 12K cDNA array (Sreenivasulu *et al.*, 2006). Samples from finger millet inflorescences were hybridized on barley seed cDNA arrays, which could explain the low number of differentially expressed genes detected. In early inflorescences of *SE7* and the wild type, 126 genes were differentially expressed at the threshold of ≥1.5-fold (four replicates, $P < 0.05$). Of these, 69 genes were up-regulated and 57 were down-regulated. A total of 17 up- and 23 down-regulated genes could not be annotated (Supplementary Table S2).

The largest set of 30 genes (40% of total) up-regulated in *SE7* inflorescences was related to transcription and translation and contained genes encoding 10 histones, nine ribosomal proteins, and several elongation and initiation factors. In contrast, only 12 genes from this category were down-regulated (Supplementary Table S2 at *JXB* online). In *SE7*, 16 up-regulated genes were related to cell proliferation, different aspects of cell wall assembly/biosynthesis, and to regulation of growth of young and meristematic tissues including floral formation (Table 1). Dynamin and α-tubulin are involved in cytokinesis and microtubule
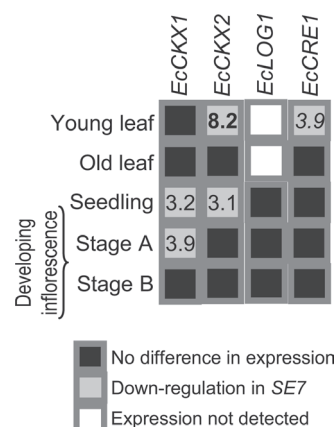

Fig. 4. Differences in expression of *EcCKX1*, *EcCKX2*, *EcLOG1*, and *EcCRE1* genes in different tissues of wild-type and *SE7* finger millet plants as analysed by qRT-PCR. Significant expression differences between SE7 and the wild type are shown by normal (*t*-test, $P < 0.05$), italic (*t*-test, $P < 0.01$), and bold (*t*-test, $P < 0.001$) numerals.

Table 1. Partial list of the genes differentially expressed in the finger millet *SE7* inflorescences compared with the wild type

Clone ID[a]	Gene identification	Blast score	Closest homologue in rice	Fold difference[b]
Genes up-regulated in the *SE7* inflorescences				
HY07H07	Peroxidase, class III	842	LOC_Os03g02920	6.86
HF04C06	Elongation factor 1β	529	LOC_Os07g42300	4.89
HY05A19	Uridylate monophosphate kinase	577	LOC_Os04g33300	4.09
HA10K05	Histone H2B-1	1540	LOC_Os01g05610	3.38
HA12L08	Poly(A)-binding protein	825	LOC_Os09g02700	3.36
HA03D02	Peroxidase II	264	LOC_Os04g59150	3.36
HA05J13	40S ribosomal protein S15A	637	LOC_Os07g10720	3.03
HB17F08	Extensin	1011	LOC_Os05g43280	3.03
HA29L06	Eukaryotic translation initiation factor 3-1α	688	LOC_Os02g02990	2.89
HB21M05	Chloroplast proteinase cnd41	2085	LOC_Os02g48900	2.82
HA01F14	Histone H4-2	1478	LOC_Os05g38740	2.81
HA11D18	Glycine-rich protein	198	LOC_Os01g15310	2.80
HY10A12	60S ribosomal protein L3	770	LOC_Os11g06750	2.72
HY07G20	Nodulin	649	LOC_Os05g01580	2.58
HB19G05	Argonaute AGO1	570	LOC_Os01g16870	2.37
HA08C04	60S ribosomal protein L11-1	989	LOC_Os04g51630	2.34
HY08K24	40S ribosomal protein S20	633	LOC_Os06g04290	2.12
HA23C20	ATP synthase γ subunit, mitochondrial	748	LOC_Os05g45740	2.10
HY10P24	MYB TF Always Early (ALY/Lin-9)	432	LOC_Os03g43800	2.04
HB13O10	Outer envelope membrane protein OEP75	284	LOC_Os02g10260	1.99
HZ61A07	Acidic ribosomal protein P2	903	LOC_Os01g09510	1.94
HY10K07	Heterotrimeric G protein, α subunit	287	LOC_Os05g27520	1.88
HB11P08	Dynamin	517	LOC_Os03g50520	1.84
HY10L09	Choline kinase	815	LOC_Os01g08760	1.78
HA29K04	Nucleolar protein 5A	187	LOC_Os07g46720	1.72
HB03J03	DEAD-Box RNA helicase	302	LOC_Os07g05050	1.70
HA14I09	α-Tubulin	1576	LOC_Os11g14220	1.68
HB14O18	Elongation factor 2	2087	LOC_Os02g32030	1.68
HF06L15	γ-Glutamyl hydrolase	424	LOC_Os05g44130	1.68
HB11K04	ATP synthase β subunit, mitochondrial	1504	LOC_Os05g47980	1.62
HA13H05	Seryl-tRNA synthetase	276	LOC_Os11g39670	1.62
HB05B24	Purple acid phosphatase 1	1105	LOC_Os03g13540	1.61
HY04C14	Glycosyl hydrolase 5, cellulase	1138	LOC_Os02g28040	1.58
HB28B23	Lipase class 3	1402	LOC_Os04g40510	1.57
HA31P02	ADP-ribosylation factor	673	LOC_Os05g41060	1.55
Genes down-regulated in *SE7* inflorescences				
HA22P12	Microsomal signal peptidase	263	LOC_Os09g38370	−12.72
HY10P05	Heat shock protein HSP80	1144	LOC_Os08g39140	−4.10
HZ57F19	Endoplasmic reticulum ATPase	335	LOC_Os10g30580	−3.29
HY10H24	DnaK-type molecular chaperone HSP70	1142	LOC_Os11g47760	−2.92
HZ65I21	Histone H2A	890	LOC_Os03g17100	−2.87
HF15K21	Peptide chain release factor subunit 1–3	513	LOC_Os03g49580	−2.78
HA06A05	Alcohol dehydrogenase 1	389	LOC_Os08g01760	−2.77
HA28N18	Chaperone DnaJ-like protein	585	LOC_Os03g57340	−2.57
HZ59A18	Ubiquitin-associated (UBA) protein	819	LOC_Os02g38050	−2.34
HB04C08	Cap-binding protein nCBP	320	LOC_Os03g15590	−2.32
HZ48I16	Phytochelatin synthetase	809	LOC_Os05g32110	−2.23
HY10N19	Elongation factor 1α	3735	LOC_Os03g08010	−2.12
HF05E04	SUMO-activating enzyme 2 (SAE2)	1394	LOC_Os05g32110	−2.06
HY06G19	Ubiquitin	2693	LOC_Os07g39780	−2.05
HY09G12	DNA repair helicase XPB1	238	LOC_Os01g49680	−2.04
HY10G03	Enolase	857	LOC_Os06g46770	−1.95
HZ57O13	Ubiquitin-activating enzyme E1	704	LOC_Os01g42850	−1.89
HB17M09	BRI1-interacting protein	309	LOC_Os03g58480	−1.82
HB06H23	Actin-related protein 2/3	858	LOC_Os01g46580	−1.78
HB30D08	Zinc carboxypeptidase	643	LOC_Os02g02710	−1.61
HB31J16	Quinone reductase	888	LOC_Os05g24880	−1.60
HF21C12	GAPDH, cytosolic	614	LOC_Os08g03290	−1.59

Table 1. Continued

Clone ID[a]	Gene identification	Blast score	Closest homologue in rice	Fold difference[b]
Genes up-regulated in the *SE7* inflorescences				
HF02G08	Glutamate decarboxylase GAD1	809	LOC_Os08g36320	−1.57
HB02N21	Brassinosteroid-insensitive 1 (BRI1)	83	LOC_Os11g39370	−1.55

a Clone ID is taken from http://pgrc.ipk-gatersleben.de/est/index.php. The full list of differentially regulated genes is given in Supplementary Table S1 at *JXB* online.

b A positive value indicates gene up-regulation in *SE7* inflorescences, and a negative value indicates gene down-regulation.

formation. Uridine monophosphate kinase is engaged in pyrimidine biosynthesis. γ-Glutamyl hydrolase sustains folate homeostasis and one-carbon metabolism necessary for nucleotide biosynthesis and methylation reactions occurring during cell wall formation (Loizeau *et al*., 2008). Extensins and glycine-rich proteins represent common structural cell wall proteins. Two peroxidases can potentially polymerize cell wall lignin (Fagerstedt *et al*., 2010). ADP-ribosylation factors are involved in vesicle and metabolite transport towards the cell wall. Nodulin 21 (MtM21) represents a potential tonoplast metabolite exporter. The respective mutants show defective cell wall formation and elongation (Ranocha *et al*., 2010). Choline kinase is involved in phospholipid biosynthesis. Purple acid phosphatase mediates phosphate acquisition and redistribution, which is important for efficient growth. Its overexpression in *Arabidopsis* results in higher seed yield (Sun *et al*., 2012). Heterotrimeric G-protein modulates cell proliferation, which is reduced in the respective null mutants (Ullah *et al*., 2001). In contrast, from this category, only an actin-related protein was down-regulated in *SE7*. Two up-regulated genes in *SE7* participate in floral formation. Argonaute 1 regulates the temporal programme of floral stem cells (Ji *et al*., 2011). ALWAYS EARLY (ALY2/Lin-9) contains Myb domains, is nuclear localized, and regulates germ-like specific gene expression in *Drosophila* with presumed similar functions in plants (Bhatt *et al*., 2004; Doggett *et al*., 2011). Three up-regulated genes in *SE7* are associated with protein or lipid degradation and another two with mitochondrial energy production.

From the genes down-regulated in *SE7* inflorescences, eight are related to pathogen defence and stress response (Table 1). Among them are three heat shock proteins, alcohol dehydrogenase, and phytochelatin synthase. Five down-regulated genes are involved in regulated protein degradation via the ubiquitin pathway. *Brassinosteroid insensitive 1* (BRI1) together with a BRI1-interacting protein is also transcriptionally down-regulated. The former encodes a leucine-rich repeat receptor-like kinase recognizing brassinosteroids, which are engaged in cell elongation. Interestingly, attenuating brassinosteroid signalling in *Arabidopsis* enhances FLC expression and the late flowering autonomous pathway (Domagalska *et al*., 2007), indicating relationships between brassinosteroids and flowering. Three down-regulated genes are related to primary metabolism such as glycolysis (enolase, GAPDH) and C:N balance (glutamate decarboxylase).

In summary, differential gene expression suggests that *SE7* young inflorescences possess a prolonged proliferation phase characterized by up-regulated transcription and translation, cell division, floral formation, and energy production. In contrast, wild-type inflorescences are similar to a more

differentiated status characterized by regulated protein degradation, brassinosteroid-mediated cell elongation, and defence/stress responses.

Discussion

Plants regenerated *in vitro* from undifferentiated cells often exhibit some level of variation called somaclonal variation. Somaclonal variation in plants is caused by increased mutation rates mainly due to nucleotide substitutions and small indels during the *in vitro* regeneration process and could be provoked by exogenous growth stimulators (Jiang *et al*., 2011; Sato *et al*., 2011). Thereby, genetic modifications lead to somaclonal variations in regenerated plantlets. Here the somaclonal line *SE7* of finger millet was analysed. Compared with the wild type, this line exhibited lower plant height as well as increased numbers of inflorescences and flowers over several generations, resulting in considerably higher seed yield per plant by up to 40% in field trials. Phenotypic features of *SE7* plants, decreased CK degradation and elevated active CK content, correlate well with CK function in stimulation of meristem activity, leading to enhanced inflorescence formation and seed set.

Measurements of CK metabolites revealed iP as the major form of active CKs in developing inflorescences of finger millet, whereas iP together with tZ are major forms in *Arabidopsis* (Tokunaga *et al*., 2012). iP levels and that of the precursor iPRP are strongly increased in *SE7* inflorescences at the initiation of differentiation, but are similar to the wild type later on (Fig. 3; Supplementary Fig. S1 at *JXB* online). Increased iP levels are probably caused by attenuated degradation, as evidenced by lower gene expression of the *EcCKX1* gene in young inflorescences. Such a shift in CK homeostasis, brought about by either decreased CK degradation or enhanced biosynthesis, can excite plant productivity. Accordingly, down-regulated *CKX* gene expression lowered CK-degrading activity and increased CK levels in rice and barley and enhanced seed numbers per plant and thousand grain weight (Ashikari *et al*., 2005; Zalewski *et al*., 2010). Overexpression of *AtLOG* genes (*AtLOG2*, *AtLOG4*, and *AtLOG7*) also increased CK biosynthesis and led to more axillary stems and larger seeds (Kuroha *et al*., 2009).

It was also found that finger millet inflorescences accumulated more tZ than cZ derivatives. It was reported earlier that several species from *Arundinoideae, Panicoideae,* and *Pooideae* subfamilies of the *Poaceae* family accumulate predominantly cZ derivatives in their leaves (Gajdosova *et al*., 2011). *Eleusine coracana* belongs to the *Chloridoideae* subfamily (Glemin and

Bataillon, 2009), which is phylogenically separate from subfamilies analysed by Gajdosova *et al.* (2011), which may explain this discrepancy. Besides, the ratio between cZ and tZ derivatives may change dramatically throughout the life span of a single plant (Gajdosova *et al.*, 2011; Tarkowská *et al.*, 2012) with cZ derivatives prevalent in the developing stages associated with limited growth. Therefore, a high level of tZ derivatives might be specific for actively grown and developing finger millet inflorescences. Interestingly, the levels of cZ precursors, *cis*-zeatin riboside-phosphate and *cis*-zeatin riboside, were also increased in the *SE7* line, additionally supporting the idea that cZ can play a role in a fine-tuning regulation of reproductive development (Tarkowská *et al.*, 2012).

The *SE7* plants exhibited decreased plant height and increased seed yield mainly due to an increased number of inflorescences and grains per plant. Levels of *EcCKX1* and/or *EcCKX2* transcripts but not those of *EcLOG1* were decreased in seedlings, young developing inflorescences, and in younger but not in older leaves (Fig. 4). It is concluded that the phenotypic changes observed in the *SE7* plants are caused by decreased expression of *EcCKX1* and *EcCKX2* genes, which resulted in elevation of iP levels in actively growing tissues and as a consequence promoted maintenance and activity of vegetative and generative meristems. This assumption is further supported by enhanced expression in the *SE7* young inflorescences of genes related to transcription, translation, and cell proliferation, to different aspects of cell wall assembly/biosynthesis, and to regulation of growth of young and meristematic tissues including floral formation. Such changes indicate enhanced cell proliferation and metabolic activity in the *SE7* meristems. Accordingly, on the transcriptional level, lipid degradation and ATP production were stimulated presumably to supply energy to the metabolically more active *SE7* meristems. The expression data support the hypothesis that enhanced levels of active CKs stimulate cell proliferation in *SE7* inflorescences. Increased meristem activity would then increase flower and seed formation in *SE7* mutant plants.

Rice plants with reduced expression of *OsCKX2* also exhibit lower plant height, but this feature is caused by mutated *gibberellin-20 oxidase* (Ashikari *et al.*, 2005). Overexpression of a *LOG* isoform in *Arabidopsis* generates semi-dwarf phenotypes (Kuroha *et al.*, 2009), indicating reduced shoot apical dominance. It is unclear why plant height is reduced together with lower expression of *CKX* in *SE7* plants. Possibly, differentiation and growth of more inflorescences as highly energy-demanding process may result in suppression of the final plant height, due to the limited energy sources. *SE7* mutant finger millet seeds germinated faster and produced longer roots (Baer *et al.*, 2007), a feature also found for barley with decreased CKX activity (Zalewski *et al.*, 2010).

EcCKX1 and *EcCKX2* cDNA sequences do not differ between the wild type and *SE7* mutant, indicating that down-regulation of *EcCKX1* and *EcCKX2* genes in *SE7* occurs at the transcriptional level. CK activity is controlled by balancing its biosynthesis, catabolism, and signalling, which generates specific homeostasis for a given tissue (Sakakibara, 2006; Werner and Schmülling, 2009; Perilli *et al.*, 2010; Frebort *et al.*, 2011). Presumably, mutations of genes which are responsible for the transcriptional regulation, such as transcription factors, might cause down-regulation

of expression of CK-related genes in *SE7*, although direct evidence is lacking. However, down-regulation of *EcCRE1* gene expression together with that of *CKX* in young leaves implicates complex networks regulating CK signalling at the transcriptional level. Altogether, it seems that a mechanism leading to the increased level of cytokinins in *SE7* inflorescences most probably differs from that described by Ashikari *et al.* (2005).

This work demonstrates a good example where somaclonal rearrangements can be advantageous for agronomic application. *In vitro* plant regeneration was successfully employed to produce finger millet plants with altered hormonal status and useful agronomic properties. The somaclonal line *SE7* is now registered as a variety, Yaroslav-8, in Ukraine. Since genetic characterization of finger millet is just beginning, the genetic resource analysed here can be of great importance, especially to finger millet breeding programmes in developing countries.

Supplementary data

Supplementary data are available at JXB online.

Figure S1. Levels of cytokinins measured in young inflorescences of the *SE7* mutant and the wild type of finger millet at the stage of flower development (stage B).

Figure S2. Dendrograms of *cytokinin oxidase/dehydrogenase* (*CKX*; A) and *LONELY GUY* (*LOG*; B) genes from barley, rice, and finger millet, and genes encoding hybrid kinases (C) implicated in cytokinin signalling.

Table S1. Primers used in cloning experiments and for qRT-PCR analyses.

Table S2. Complete list of differentially expressed genes in the *SE7* finger millet inflorescences at stage A compared with the wild type, together with gene annotation, normalized gene expression values, and their statistical significance.

Acknowledgements

References

Ashikari M, Sakakibara H, Lin S, Yamamoto T, Takashi T, Nishimura A, Angeles ER, Qian Q, Kitano H, Matsuoka M. 2005. CK oxidase regulates rice grain production. *Science* **309,** 741–745.

Bayer GY, Yemets AI, Stadnichuk NA, Rakhmetov DB, Blume YB. 2007. Somaclonal variability as a source for creation of new varieties of finger millet (*Eleusine coracana* (L.) Gaertn.). *Cytology and Genetics* **41,** 204–208.

Barazesh S, McSteen P. 2008. Hormonal control of grass inflorescence development. *Trends in Plant Sciences* **13,** 656–662.

Bartrina I, Otto E, Strnad M, Werner T, Schmülling T. 2011. CK regulates the activity of reproductive meristems, flower organ size,

ovule formation, and, thus, seed yield in *Arabidopsis thaliana*. *The Plant Cell* **23,** 69–80.

Bhatt AM, Zhang Q, Harris SA, White-Cooper H, Dickinson H. 2004. Gene structure and molecular analysis of *Arabidopsis thaliana* ALWAYS EARLY homologs. *Gene* **336,** 219–229.

Bolstad BM, Irizarry RA, Astrand M, Speed TP. 2003. A comparison of normalization methods for high density oligonucleotide array data based on bias and variance. *Bioinformatics* **19,** 185–193.

Ceasar SA, Ignacimuthu S. 2011. *Agrobacterium*-mediated transformation of finger millet (*Eleusine coracana* (L.) Gaertn.) using shoot apex explants. *Plant Cell Reports* **30,** 1759–1770.

Dida MM, Srinivasachary, Ramakrishnan S, Bennetzen JL, Gale MD, Devos KM. 2007. The genetic map of finger millet, *Eleusine coracana*. *Theoretical and Applied Genetics* **114,** 321–332.

Dobrev PI, Kaminek M. 2002. Fast and efficient separation of cytokinins from auxin and abscisic acid and their purification using mixed-mode solid-phase extraction. *Journal of Chromatography A* **950,** 21–29.

Dobrev P, Motyka V, Gaudinova A, Malbeck J, Travnickova A, Kaminek M, Vankova R. 2002. Transient accumulation of *cis*- and *trans*-zeatin type cytokinins and its relation to cytokinin oxidase activity during cell cycle of synchronized tobacco BY-2 cells. *Plant Physiology and Biochemistry* **40,** 333–337.

Doggett K, Jiang J, Aleti G, White-Cooper H. 2011. Wake-up-call, a lin-52 paralogue, and Always early, a lin-9 homologue physically interact, but have opposing functions in regulating testis-specific gene expression. *Developmental Biology* **355,** 381–393.

Domagalska MA, Schomburg FM, Amasino RM, Vierstra RD, Nagy F, Davis SJ. 2007. Attenuation of brassinosteroid signaling enhances FLC expression and delays flowering. *Development* **134,** 2841–2850.

Fagerstedt KV, Kukkola EM, Koistinen VV, Takahashi J, Marjamaa K. 2010. Cell wall lignin is polymerised by class III secretable plant peroxidases in Norway spruce. *Journal of Integrative Plant Biology* **52,** 186–194.

Frébort I, Kowalska M, Hluska T, Frébortová J, Galuszka P. 2011. Evolution of cytokinin biosynthesis and degradation. *Journal of Experimental Botany* **62,** 2431–2452.

Galuszka P, Frebort I, Sebela M, Sauer P, Jacobsen S, Pec P. 2001. Cytokinin oxidase or dehydrogenase? Mechanism of cytokinin degradation in cereals. *European Journal of Biochemistry* **268,** 450–461.

Glemin S, Bataillon T. 2009. A comparative view of the evolution of grasses under domestication. *New Phytologist* **183,** 273–290.

Ji L, Liu X, Yan J, *et al.* 2011. ARGONAUTE10 and ARGONAUTE1 regulate the termination of floral stem cells through two microRNAs in Arabidopsis. *PLoS Genetics* **7,** e1001358.

Jiang C, Mithani A, Gan X, Belfield EJ, Klingler JP, Zhu JK, Ragoussis J, Mott R, Harberd NP. 2011. Regenerant Arabidopsis lineages display a distinct genome-wide spectrum of mutations conferring variant phenotypes. *Current Biology* **21,** 1385–1390.

Kamada-Nobusada T, Sakakibara H. 2009. Molecular basis for cytokinin biosynthesis. *Phytochemistry* **70,** 444–449.

Kudo T, Kiba T, Sakakibara H. 2010. Metabolism and long-distance translocation of cytokinins. *Journal of Integrative Plant Biology* **52,** 53–60.

Kurakawa T, Ueda N, Maekawa M, Kobayashi K, Kojima M, Nagato Y, Sakakibara H, Kyozuka J. 2007. Direct control of shoot meristem activity by a cytokinin-activating enzyme. *Nature* **445,** 652–655.

Kuroha T, Tokunaga H, Kojima M, Ueda N, Ishida T, Nagawa S, Fukuda H, Sugimoto K, Sakakibara H. 2009. Functional analyses of LONELY GUY cytokinin-activating enzymes reveal the importance of the direct activation pathway in Arabidopsis. *The Plant Cell* **21,** 3152–3169.

Livak KJ, Schmittgen TD. 2001. Analysis of relative gene expression data using real-time quantitative PCR and the 2(T) (–Delta Delta C) method. *Methods* **25,** 402–408.

Loizeau K, De Brouwer V, Gambonnet B, Yu A, Renou JP, Van Der Straeten D, Lambert WE, Rébeillé F, Ravanel S. 2008. A genome-wide and metabolic analysis determined the adaptive response of Arabidopsis cells to folate depletion induced by methotrexate. *Plant Physiology* **148,** 2083–2095.

Matsumoto T, Tanaka T, Sakai H, *et al.* 2011. Comprehensive sequence analysis of 24,783 barley full-length cDNAs derived from 12 clone libraries. *Plant Physiology* **156,** 20–28.

Mechael G, Seiler-Kelbitsch H. 1972. Cytokinin content and kernel size of barley grain as affected by environmental and genetic factors. *Crop Science* **12,** 162–165.

Miyawaki K, Tarkowski P, Matsumoto-Kitano M, Kato T, Sato S, Tarkowska D, Tabata S, Sandberg G, Kakimoto T. 2006. Roles of Arabidopsis ATP/ADP isopentenyltransferases and tRNA isopentenyltransferases in cytokinin biosynthesis. *Proceedings of the National Academy of Sciences, USA* **103,** 16598–16603.

Müller B. 2011. Generic signal-specific responses: cytokinin and context-dependent cellular responses. *Journal of Experimental Botany* **62,** 3273–3288.

Perilli S, Moubayidin L, Sabatini S. 2010. The molecular basis of cytokinin function. *Current Opinion in Plant Biology* **13,** 21–26.

Radchuk V, Weier D, Radchuk R, Weschke W, Weber H. 2011. Development of maternal seed tissue in barley is mediated by regulated cell expansion and cell disintegration and coordinated with endosperm growth. *Journal of Experimental Botany* **62,** 1217–1227.

Ramakers C, Ruijter JM, Deprez RHL, Moorman AFM. 2003. Assumption-free analysis of quantitative real-time polymerase chain reaction (PCR) data. *Neuroscience Letters* **339,** 62–66.

Ranocha P, Denancé N, Vanholme R, *et al.* 2010. Walls are thin 1 (WAT1), an Arabidopsis homolog of Medicago truncatula NODULIN21, is a tonoplast-localized protein required for secondary wall formation in fibers. *The Plant Journal* **63,** 469–483.

Sakakibara H. 2006. Cytokinins: activity, biosynthesis, and translocation. *Annual Review of Plant Biology* **57,** 431–449.

Sakamoto T, Sakakibara H, Kojima M, Nagasaki H, Yamamoto Y, Inukai Y, Sato Y, Matsuoka M. 2006. Ectopic expression of KNOTTED1-like homeobox protein induces expression of cytokinin biosynthesis genes in rice. *Plant Physiology* **142,** 54–62.

Sato M, Hosokawa M, Doi M. 2011. Somaclonal variation is induced *de novo* via the tissue culture process: a study quantifying mutated cells in *Saintpaulia*. *PLoS One* **6,** e23541.

Schmülling T, Werner T, Riefler M, Krupková E, Manns IB. 2003. Structure and function of cytokinin oxidase/dehydrogenase genes of maize, rice, Arabidopsis and other species. *Journal of Plant Research* **116,** 241–252.

Séguéla M, Briat JF, Vert G, Curie C. 2008. Cytokinins negatively regulate the root iron uptake machinery in Arabidopsis through a growth-dependent pathway. *The Plant Journal* **55,** 289–300.

Sreenivasulu N, Radchuk V, Strickert M, Miersch O, Weschke W, Wobus U. 2006. Gene expression patterns reveal tissue-specific signaling networks controlling programmed cell death and ABA-regulated maturation in developing barley seeds. *The Plant Journal* **47,** 310–327.

Srinivasachary, Dida MM, Gale MD, Devos KM. 2007. Comparative analyses reveal high levels of conserved colinearity between the finger millet and rice genomes. *Theoretical and Applied Genetics* **115,** 489–499.

Sun F, Suen PK, Zhang Y, Liang C, Carrie C, Whelan J, Ward JL, Hawkins ND, Jiang L, Lim BL. 2012. A dual-targeted purple acid phosphatase in *Arabidopsis thaliana* moderates carbon metabolism and its over-expression leads to faster plant growth and higher seed yield. *New Phytologist* **194,** 206–219.

Takei K, Yamaya T, Sakakibara H. 2004. Arabidopsis CYP735A1 and CYP735A2 encode cytokinin hydroxylases that catalyze the biosynthesis of *trans*-zeatin. *Journal of Biological Chemistry* **279,** 41866–41872.

Tarkowská D, Filek M, Biesaga-Kościelniak J, Marcińska I, Macháčková I, Krekule J, Strnad M. 2012. Cytokinins in shoot apices of *Brassica napus* plants during vernalization. *Plant Science* **187,** 105–112.

Tokunaga H, Kojima M, Kuroha T, Ishida T, Sugimoto K, Kiba T, Sakakibara H. 2012. Arabidopsis lonely guy (LOG) multiple mutants reveal a central role of the LOG-dependent pathway in CK activation. *The Plant Journal* **69,** 355–365.

Udvardi MK, Czechowski T, Scheible WR. 2008. Eleven golden rules of quantitative RT-PCR. *The Plant Cell* **20,** 1736–1737.

Ullah H, Chen JG, Young JC, Im KH, Sussman MR, Jones AM. 2001. Modulation of cell proliferation by heterotrimeric G protein in Arabidopsis. *Science* **292,** 2066–2069.

Werner T, Motyka V, Laucou V, Smets R, Van Onckelen H, Schmülling T. 2003. Cytokinin-deficient transgenic Arabidopsis plants show multiple developmental alterations indicating opposite functions of cytokinins in the regulation of shoot and root meristem activity. *The Plant Cell* **15,** 2532–2550.

Werner T, Nehnevajova E, Kollmer I, Novak O, Strnad M, Kramer U, Schmülling T. 2010. Root-specific reduction of cytokinin causes enhanced root growth, drought tolerance, and leaf mineral enrichment in Arabidopsis and tobacco. *The Plant Cell* **22,** 3905–3920.

Werner T, Schmülling T. 2009. Cytokinin action in plant development. *Current Opinion in Plant Biology* **12,** 527–538.

Yemets AI, Bayer GY, Klimkina LA, Stadnichuk NA, Abramov AA. 2003. Cultivation and regeneration in vitro of finger millet plants Eleusine coracana (L.) Gaertn. var. Tropikanka. *Physiology and Biochemistry of Cultivated Plants* **35,** 152–159 (in Russian).

Zalewski W, Galuszka P, Gasparis S, Orczyk W, Nadolska-Orczyk A. 2010. Silencing of the *HvCKX1* gene decreases the cytokinin oxidase/dehydrogenase level in barley and leads to higher plant productivity. *Journal of Experimental Botany* **61,** 1839–1851.

Zhang H, Sreenivasulu N, Weschke W, *et al.* 2004. Large-scale analysis of the barley transcriptome based on expressed sequence tags. *The Plant Journal* **40,** 276–290.